Progress In Electromagnetics Research C, Vol. 12, 37–51, 2010

A MODIFIED FRACTAL RECTANGULAR CURVE DIELECTRIC RESONATOR ANTENNA FOR WIMAX APPLICATION

R. K. Gangwar and S. P. Singh

Department of Electronics Engineering
Institute of Technology, Banaras Hindu University
Varanasi 221005, India

D. Kumar

Department of Ceramic Engineering
Institute of Technology, Banaras Hindu University
Varanasi 221005, India

Abstract—This paper presents the simulation study of a wideband modified fractal rectangular curve iteration-1 (FRC-1) dielectric resonator antenna (DRA) along with conventional FRC DRAs of different iteration levels for WiMAX application. The simulation study has been carried out using CST Microwave Studio software. The design procedure and radiation performance characteristics of modified and conventional FRC DRAs are described and the simulation results for modified FRC-1 DRA are compared with those of a conventional FRC-1 DRA of identical outer dimensions. The simulation results for the material dielectric constant dependent radiation characteristics of both the FRC-1 DRAs are also presented. The results presented here may be useful in designing portable personnel communication device antennas and in analyzing the performance of these antennas for wireless communication.

1. INTRODUCTION

The dielectric resonator (DR) is fabricated from a dielectric material having low-loss ($\tan\delta \approx 10^{-4}$, or less) and high dielectric constant ($\varepsilon_r \approx 10 - 100$). Its resonant frequency is predominantly a function of size, shape, and material permittivity. DRs offer the advantages of

Corresponding author: R. K. Gangwar (ravi.gangwar.ece07@itbhu.ac.in).

small size, lightweight, low profile, and low cost. When a dielectric resonator is not entirely enclosed by a conducting boundary, it can radiate, and becomes an antenna, named Dielectric resonator antenna (DRA). DRAs have several desirable antenna features including high radiation efficiency, flexible feed arrangement, simple geometry, and compactness [1–4]. The DRAs provide wider bandwidth, higher efficiency with better power handling capability and don't support surface waves as compared with the microstrip antenna. They might be useful in a variety of personal portable wireless devices and mobile communication and tactical systems such as radars [5].

Various DRA modes can be excited using different excitation techniques, such as the conducting probe, microstrip line, slot, co-planar waveguide etc. DRAs are available in various basic classical shapes such as rectangular, cylindrical, spherical and hemispherical geometries. Rectangular DRAs can be designed with greater flexibility since two of the three of its dimensions can be varied independently for a fixed resonant frequency and known dielectric constant of the material [6].

Fractal-shaped antennas show some interesting features that stalk from their inherent geometrical properties. The self-similarity of certain fractal geometries result in wideband behavior of these types of fractal antennas. From another point of view, high convoluted shape and space-filling properties of certain fractals allow to reduce volume occupied by a resonant element. Although complex objects with similar properties of the fractals could be defined, the use of fractal geometries has the advantage that irregular complex objects can be described in a well defined geometrical framework [5].

Numerous techniques have been used to improve the bandwidth of the dielectric resonator antennas such as introduction of fractal geometry, change in aspect ratio of DRA and by varying dielectric constant of DRA material [7, 8]. With the use of lower material dielectric constant ($5 \leq \varepsilon_r \geq 20$) along with proper choice of dimensions of the structure the radiation field can be enhanced over wide band [3, 9]. Material dielectric constant 8/10 has been used for wideband dielectric resonator antennas [10, 11]. Many low loss materials having dielectric constant of 8 and 20 are listed in reference [12].

In the light of foregoing discussion wideband modified fractal rectangular curve, iteration-1 (FRC-1) dielectric resonator antennas (DRAs) have been proposed for WiMAX applications. The modified FRC-1 DRA consists of an FRC-1 DRA with a cylindrical hole in its centre. The performance characteristics of the proposed modified FRC-1 DRA and conventional FRC DRAs of different iteration levels

obtained through simulation studies using CST Microwave Studio software are described. The radiation characteristics of modified FRC-1 DRA are compared with those of conventional FRC-1 DRA of identical outer dimensions. The effect of material dielectric constant on the radiation characteristics of the proposed FRC-1 DRA and conventional FRC-1 DRA is also investigated.

2. THE FRACTAL RECTANGULAR CURVE DIELECTRIC RESONATOR ANTENNA

The shape of the proposed configuration originates from the "Squares Curve" [13], using a rectangular initiator instead of a square one and named after this as a Fractal Rectangular Curve (FRC). The FRC geometry was firstly proposed as a microstrip patch antenna radiator in [14]. It is constructed by applying a geometric transformation on the rectangle FRC-0 (initiator) of Fig. 1. By producing four more rectangles of a quarter of the area of FRC-0 and placing them at the four corners of the initiator as depicted in Fig. 1, the pre-fractal FRC-1 is obtained. Repeating this adding procedure one more time at each rectangle placed at the four corners results in the pre-fractal FRC-2 (Fig. 1) [14]. Coaxial probe coupling is chosen for exciting each of the FRC DRAs.

Each of the four dielectric resonator antennas of Fig. 1 is assumed to reside on a ground plane of dimensions 50 mm × 50 mm. The rectangular dielectric resonator antenna with relative permittivity of dielectric, $\varepsilon_r = 20$ and dielectric loss ($\tan\delta = 1 \times 10^{-4}$) and having dimensions: length = 20 mm, width = 12 mm and height = 13 mm is chosen so that it resonates at 2.65 GHz.

The initiator of FRC DRA shown in Fig. 1 has dimensions denoted as a_0 (length), b_0 (width), h_0 (height), D_0 (semi-diagonal) and A_0 (surface area). Each iteration increases the semi-diagonal dimension, the perimeter and the rectangular area enclosing the figure. The semi-diagonal dimension of the antenna at the nth iteration is found to be:

$$D_n = \sum_{i=0}^{n} \frac{1}{2^{i+1}} \sqrt{a_0^2 + b_0^2} \quad \text{Or} \quad D_n = 2D_0 \sum_{i=0}^{n} \frac{1}{2^{i+1}} \tag{1}$$

The surface area of the antenna structure is given by:

$$A_n = \sum_{i=0}^{n} \left(\frac{3}{4}\right)^i \left(a_0 b_0 + (b_0 h_0 + a_0 h_0) \left[\left(\frac{3}{2}\right)^i - \frac{1}{2}\right] \times 4\right) \tag{2}$$

Theoretically as n tends to infinity the semi-diagonal of the FRC is doubled, the perimeter goes to infinity, while the surface area increases four times.

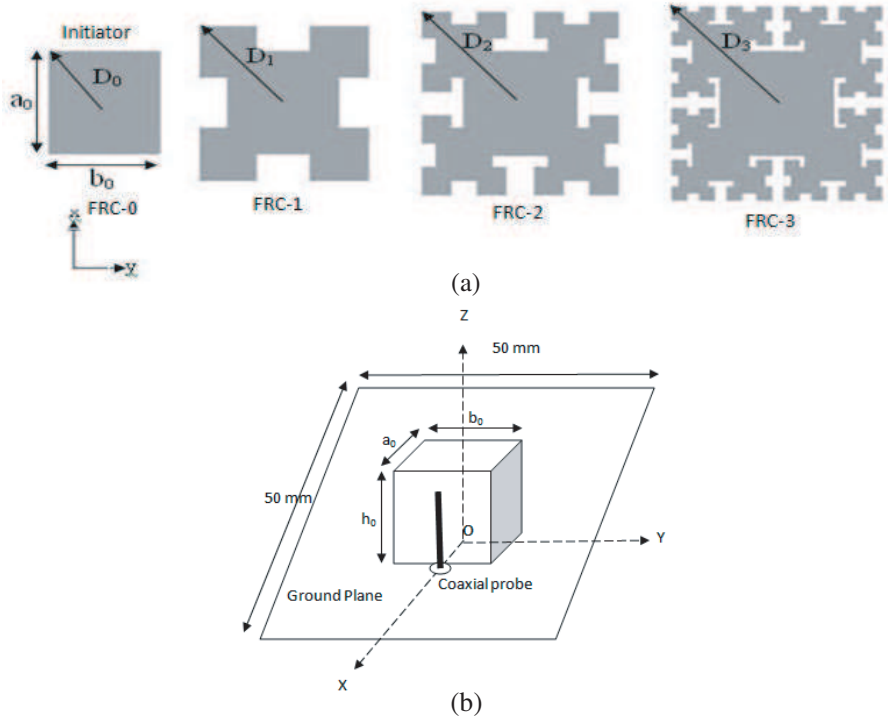

Figure 1. Construction of the fractal rectangular curve dielectric resonator antenna. (a) 2D view. (b) 3D view of initiator (FRC-0).

It is worth mentioning here that the Q-factor of a cavity is proportional to its volume and is inversely proportional to its area. Therefore, in DRA, when fractal iteration level increases, the ratio of surface/volume increases and the radiation Q-factor, which is $Q_{rad} = \frac{\omega_r W}{P_{rad}}$ decreases. Consequently, the bandwidth of DRA increases since bandwidth (BW) given by the following expression is inversely proportional to the radiation Q-factor (Q_{rad}):

$$\text{BW} = \frac{\text{VSWR} - 1}{Q_{rad}\sqrt{\text{VSWR}}} \qquad [5] \tag{3}$$

3. MESHING AND BOUNDARY CONDITIONS

Due to the fact that a computer is only capable of providing solutions of problems in a region of finite dimensions, boundary conditions need to be satisfied. This can be done by opening the dialog box entitled

'Boundary Conditions' in the CST Microwave Studio software. Under this dialogue box the 'boundaries' property sheet is entered for the structure to be modeled. The structure is then displayed with a boundary box coloured at each boundary. Two boundary types are used here, first one is 'electric': It operates like a perfect electric conductor, i.e., all tangential electric fields and normal magnetic fluxes are set to zero and second is 'open' (PML): It operates like free space, i.e., waves can pass this boundary with minimal reflections. These two boundary conditions are applicable to six faces of the projects bounding box (xmin/xmax/ymin/ymax/zmin/zmax) as shown in Fig. 2 [15].

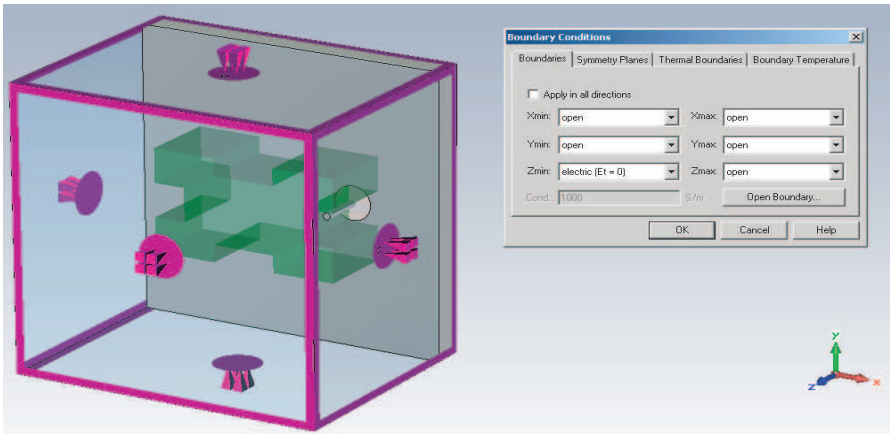

Figure 2. Boundary conditions with boundary box of the FRC-1 DRA.

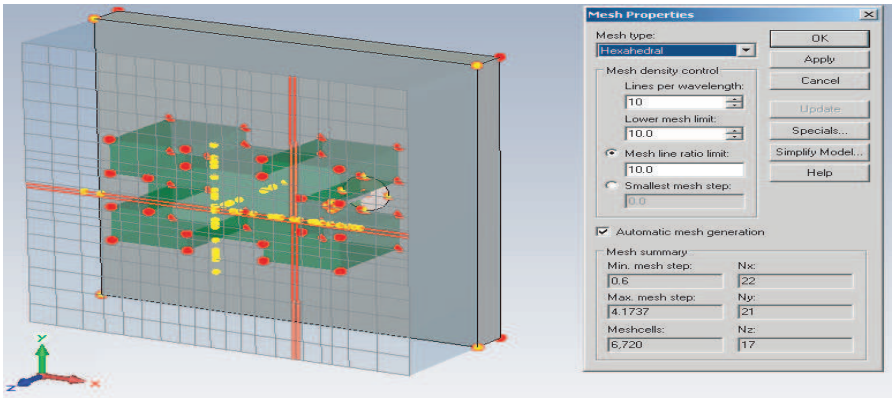

Figure 3. Mesh view with mesh properties of the FRC-1 DRA.

CST uses the Finite Integration Method which requires the computational domain to be covered by a hexahedral mesh. Hexahedral meshing used here is very robust even for most complex imported geometries and provide very fast computations. In Fig. 3, red dot is a mesh node at a particular position. The mesh lines pass through such mesh nodes. A density point (yellow dot) acts as a control point at which the mesh density may change and is used to refine the mesh within important regions. On the other hand, 'density control' points are inserted to reduce the mesh density in less important domains. The cross-sectional area of red lines shows the 'smallest mesh step'. Lines per wavelength with 'lower mesh limit' defines the size of 'maximum mesh step' and 'mesh line ratio limit' with 'smallest mesh step' defines the limitation for the smallest mesh step [15].

4. SIMULATION RESULTS AND DISCUSSION

4.1. Return Loss and Input Impedance Characteristics

4.1.1. Conventional FRC DRAs

A $50\,\Omega$ coaxial probe situated at the edge of right middle portion is used to excite $\mathrm{TE}^{y}_{1\delta 1}$ mode in each of the conventional FRC DRAs of iteration levels '0', '1', '2' and '3' as shown in Fig. 1(b). The length of probe from the surface of ground plane facing each FRC DRA is optimized using CST Microwave Studio software to provide minimum return loss at the resonant frequency. The simulation study of return loss and input impedance vs. frequency characteristics of conventional FRC DRAs with material dielectric constant $\varepsilon_r = 20$ and dielectric loss ($\tan\delta = 1 \times 10^{-4}$) for different fractal iteration levels has been carried out using CST Microwave Studio software. The simulation results for variation in return loss and input impedance vs. frequency are given in Figs. 4 and 5 respectively.

From Figs. 4, 5 and Table 1, it can be seen that resonant frequency of FRC DRA shows a decreasing trend with increase in iteration level. The decrease in resonant frequency with increase in iteration level is due to increase in the volume of dielectric resonator as the iteration level increases. This behavior is similar to the performance of microtsrip FRC patch antenna when iteration level increases [14]. Also, the return loss of FRC DRA at resonance also decreases with increase in iteration level up to iteration level 2. The $-10\,\mathrm{dB}$ bandwidth of FRC DRA increases with increase in iteration number. The increase in return loss bandwidth with the iteration level may be due to increase in surface to volume ratio of the structure and hence increase in loss due to radiation from the antenna.

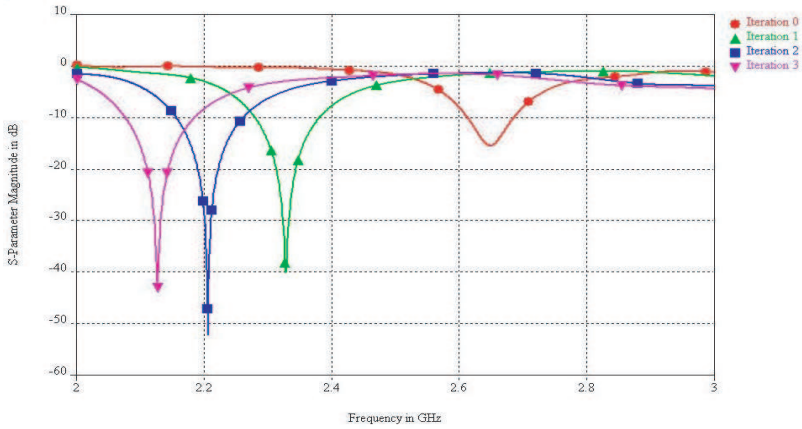

Figure 4. Variation in return loss with frequency for conventional FRC DRAs.

Table 1. Simulated performance of conventional FRC DRAs.

Parameters	**Iteration 0**	**Iteration 1 (1st order)**	**Iteration 2 (2nd order)**	**Iteration 3 (3rd order)**
Resonant frequency in GHz	2.649	2.329	2.207	2.128
Operating frequency range ($\|S_{11}\| = 10$ dB)	2.6843–2.6143 GHz	2.381–2.2821 GHz	2.2607–2.1583 GHz	2.381–2.0786 GHz
Return loss bandwidth in %	2.619	4.246	4.639	4.976

From Fig. 5, it can be observed that for each iteration the frequency at which input resistance becomes maximum is slightly lower than that at which input reactance becomes zero. This may be due to the effect of coaxial feed inductance. The input reactance is assumed to be zero at the resonant frequency of the structure. It can be seen from Fig. 5 that input resistance at resonance first reduces and then increases with increase in iteration level.

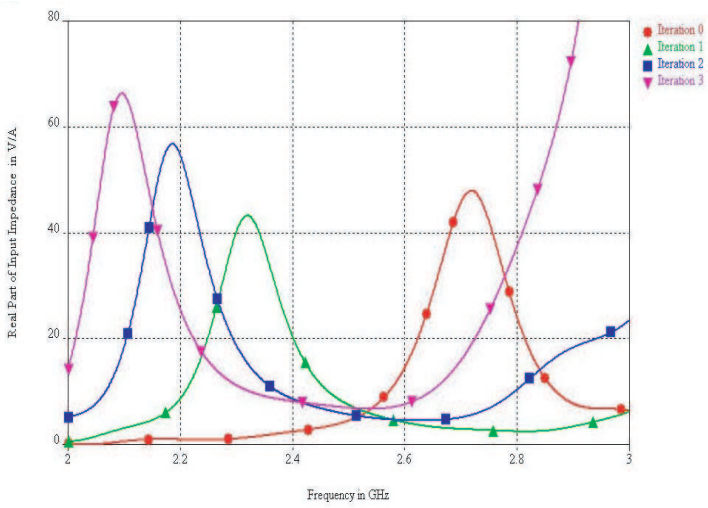

(a)

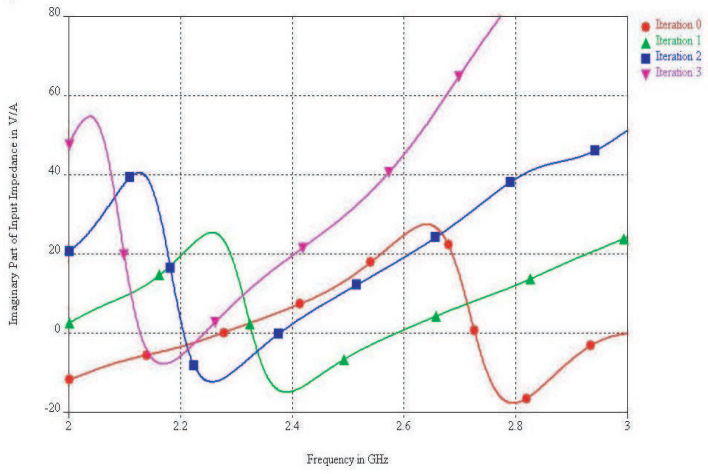

(b)

Figure 5. Variation in input impedance with frequency for conventional FRC DRAs. (a) Real part. (b) Imaginary part.

4.1.2. Modified FRC-1 DRA and Comparison with Conventional FRC-1 DRA

The geometry of FRC DRA (iteration 1) called FRC-1 DRA is modified by introduction of a hole at its centre (Fig. 6). A 50 Ω coaxial probe is used to excite $TE^{y}_{1\delta 1}$ mode in the modified FRC

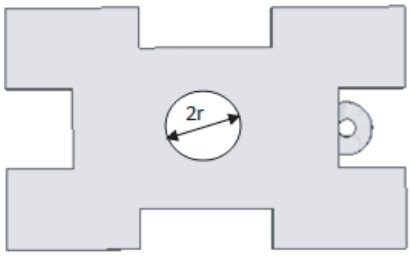

Figure 6. Geometry of modified FRC-1 DRA.

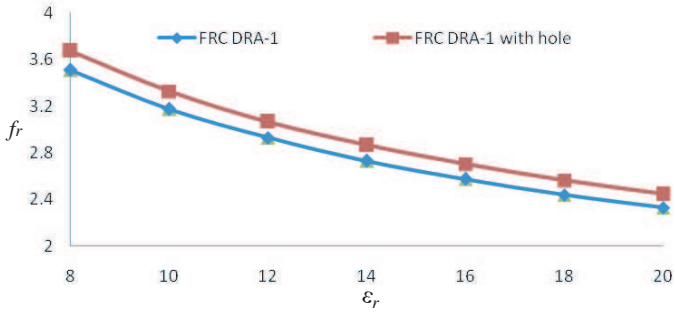

Figure 7. Effect of material dielectric constant on resonant frequency of conventional and modified FRC-1 DRAs.

DRA from the edge of right middle portion as shown in Fig. 6. The length of coaxial probe from the surface of ground plane is optimized using CST Microwave Studio software to obtain minimum return loss at the corresponding resonant frequency. The variations in resonant frequency and percentage return loss bandwidth versus material dielectric constant of modified and conventional FRC-1 DRAs obtained through simulation are presented in Figs. 7 and 8. The parameters extracted from Figs. 7 and 8 for material dielectric constant values of 8 and 20 are given in Table 2 keeping constant dielectric loss ($\tan\delta = 1 \times 10^{-4}$). It can be observed from Figs. 7, 8 and Table 2 that both resonant frequency and percentage bandwidth reduce with increase in material dielectric constant for both modified and conventional FRC-1 DRAs. Also for a given material dielectric constant the resonant frequency of modified FRC-1 DRA is higher than that of conventional FRC-1 DRA due to less material volume present in modified structure. The -10 dB return loss bandwidth of modified FRC-1 DRA is wider than that of conventional FRC-1 DRA due to larger surface-to-volume ratio and hence greater radiation loss from the modified structure.

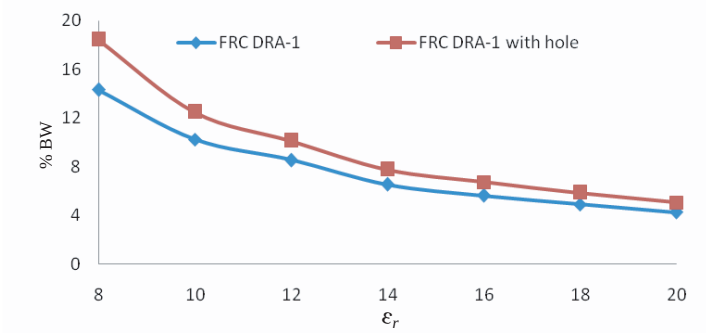

Figure 8. Effect of material dielectric constant on percentage return loss bandwidth of conventional and modified FRC-1 DRAs.

Table 2. Simulated resonance performance of conventional and modified FRC-1 DRA.

Parameters	**Conventional FRC-1 DRA**		**Modified FRC-1 DRA**	
	$\varepsilon_r = 20$	$\varepsilon_r = 8$	$\varepsilon_r = 20$	$\varepsilon_r = 8$
Resonant frequency in GHz	2.329	3.51	2.444	3.674
Operating frequency range in GHz ($\lvert S_{11}\rvert = 10\,\text{dB}$)	2.381–2.2821	3.2967–3.8	2.3845–2.5083	3.4056–4.831
Return loss bandwidth in %	4.246	14.339	5.065	18.44

The effect of the diameter of centrally located hole present in modified FRC-1 DRA of Fig. 6 on the return loss vs. frequency performance is shown in Fig. 9. It can be seen from Fig. 9 that $-10\,\text{dB}$ return loss bandwidth increases with increase in the diameter of cylindrical hole present in modified FRC-1 DRA. This is due to the increase in effective surface area-to-volume ratio of the structure which provides more radiation loss.

The simulation results for input impedance vs. frequency characteristics of modified FRC-1 DRA for material dielectric constant $\varepsilon_r = 8$ and 20 are presented in Fig. 10. Also shown in Fig. 10 are the results for conventional FRC-1 DRA for comparison. From Fig. 10, it

can be observed that the frequency at which input resistance becomes maximum is slightly lower than that at which input reactance becomes zero. This may be due to the effect of coaxial feed inductance. The input reactance is assumed to be zero at the resonant frequency of the structure. The maximum values of resistance of modified FRC-1 DRA for material dielectric constant $\varepsilon_r = 8$ and 20 are respectively equal to 66.68 Ω and 66.69 Ω. The corresponding resistance value of conventional FRC-1 DRA is 66.11 Ω and 42.57 Ω.

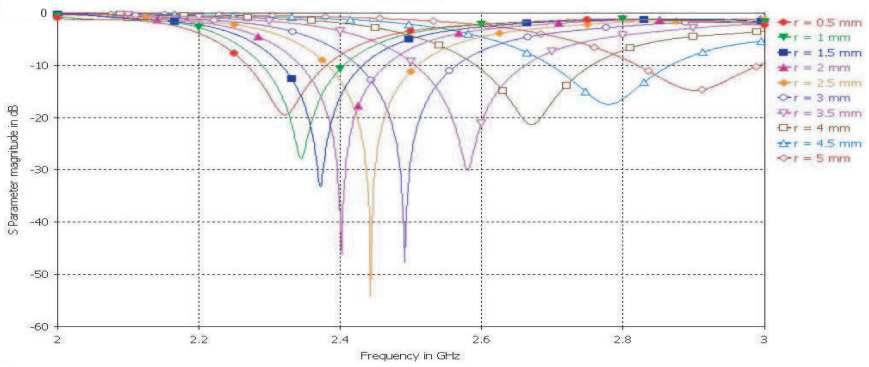

Figure 9. Effect of cylindrical hole diameter on return loss vs. frequency characteristics of modified FRC-1 DRA with $\varepsilon_r = 20$.

Table 3. Far field parameters of conventional and modified FRC-1 DRAs.

Far Field Parameters	**Conventional FRC-1 DRA**		**Modified FRC-1 DRA**	
	$\varepsilon_r = 20$	$\varepsilon_r = 8$	$\varepsilon_r = 20$	$\varepsilon_r = 8$
Directivity in dBi	5.039	5.747	5.22	6.009
Gain in dB	5.019	5.736	5.176	5.998
Radiation efficiency in %	98.36	99.75	98.99	99.76
3-dB Beam-width in deg. (Y-Z plane)	100.6	121.6	102.3	127.5

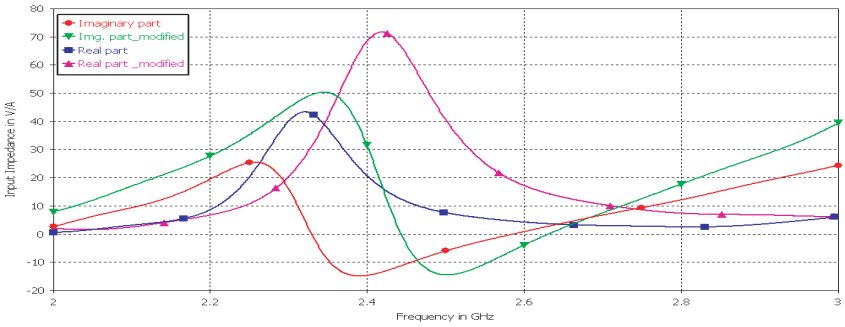

(a)

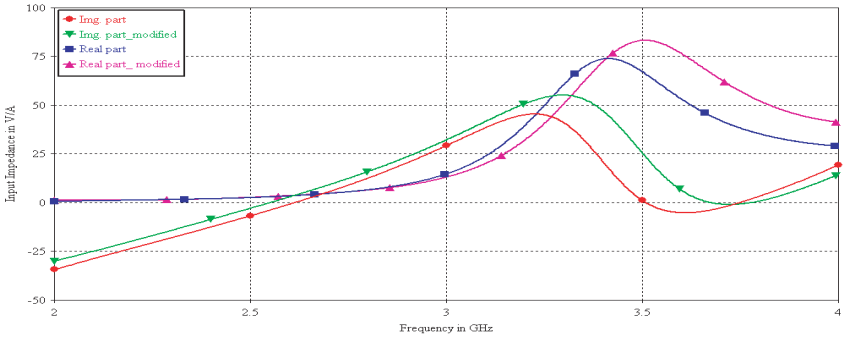

(b)

Figure 10. Variation of input impedance with frequency for conventional FRC-1 DRA and modified FRC-1 DRA. (a) with $\varepsilon_r = 20$, (b) with $\varepsilon_r = 8$.

4.2. Far Field Pattern

The far field patterns of conventional and modified FRC-1 DRAs having material dielectric constants $\varepsilon_r = 8$ and 20 at their respective resonant frequencies are studied through simulation using CST Microwave Studio software. The far field patterns of these antennas for material dielectric constant $\varepsilon_r = 8$ and 20 are presented in Figs. 11 and 12 respectively. The far field parameters of modified and conventional FRC-1 DRAs extracted from Figs. 11 and 12 are given in Table 3.

From Figs. 11, 12 and Table 3, it can be seen that modified and conventional FRC-1 DRAs have broadside patterns. The beams in X-Z and X-Y planes of the both antennas are almost omni-directional. For a given material dielectric constant the values of gain, directivity, radiation efficiency and beam-width in Y-Z plane are higher in case of modified FRC-1 antenna. This may be due to larger surface area for radiation in case of modified structure. These results corroborate our

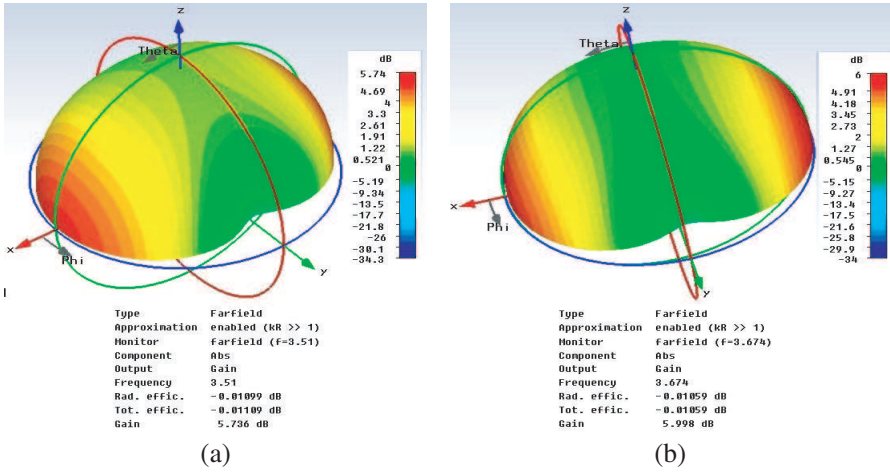

Figure 11. Radiation patterns (3D Views) of FRC-1 DRAs with $\varepsilon_r = 8$. (a) Conventional FRC DRA. (b) Modified FRC-1 DRA.

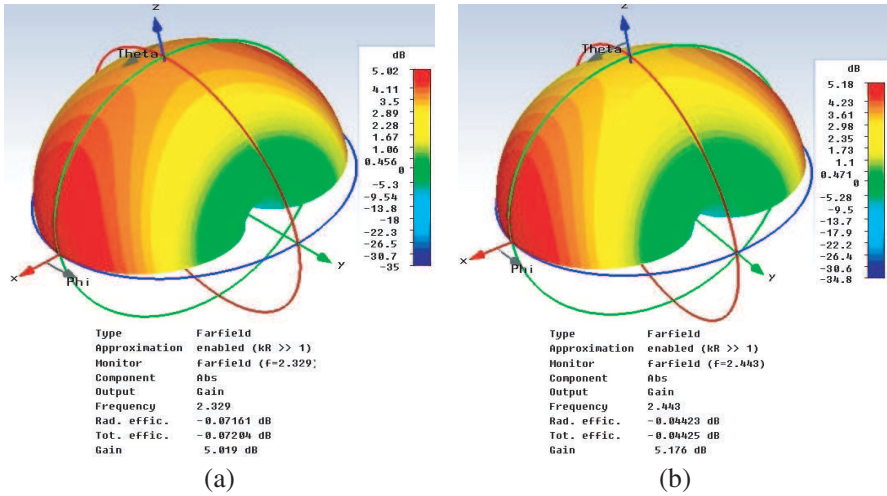

Figure 12. Radiation patterns (3D Views) of FRC-1 DRAs with $\varepsilon_r = 20$. (a) Conventional FRC DRA. (b) Modified FRC-1 DRA.

earlier finding that modified antenna provides higher input resistance at resonance as compared with conventional antenna. The trend of variation in the results when material dielectric constant ε_r is reduced looks similar to that obtained in going from conventional to modified antenna but the values of parameters increase by significant amount

when ε_r is reduced from 20 to 8. This may be due to the fact that the wave becomes loosely bound to the ceramic material as dielectric constant reduces and hence there is greater chance for radiation to take place.

5. CONCLUSION

A wideband modified FRC-1 DRA with improved gain, bandwidth and radiation efficiency for WiMAX application has been proposed in this paper. The radiation characteristics of the proposed modified FRC-1 DRA have been obtained through simulation using CST Microwave Studio software and compared with those of conventional FRC-1 DRA. The effect of change in material dielectric constant on the bandwidth and other radiation parameters of modified as well as conventional antennas have also been investigated. The results presented here may be useful in designing wideband DRAs and in analyzing their performance for WiMAX application.

REFERENCES

1. Mongia, R. K. and P. Bhartia, "Dielectric resonator antennas — A review and general design relation for resonant frequency and bandwidth," *International Journal of Microwave and Millimeter Wave Computer-aided Engineering*, Vol. 4, 230–247, 1994.
2. Ittipiboon, A. and R. K. Mongia, "Theoretical and experimental investigations on rectangular dielectric resonator antennas," *IEEE Trans. on Antennas and Propagation*, Vol. 45, 1348–1356, 1997.
3. Rezaei, P., M. Hakkak, and K. Forooaghi, "Design of wide-band dielectric resonator antenna with a two-segment structure," *Progress In Electromagnetics Research*, PIER 66, 111–124, 2006.
4. Kajfez, D. and A. A. Kishk, "Dielectric resonator antenna — possible candidate for adaptive antenna arrays," *Telecommunications, Next Generation Networks and Beyond International Symposium*, Portoroz, Slovenia, May 2002.
5. Hajihasemi, M. R. and H. Abiri, "Prametric study of novel types of dielectric resonator antennas based on fractal geometry," *International Journal of RF and Microwave Computer-aided Engineering*, Vol. 17, No. 4, 416–424.
6. Saed, M. and R. Yadla, "Microstrip-fed low profile and compact dielectric resonator antennas," *Progress In Electromagnetics Research*, PIER 56, 151–162, 2006.

7. Werner, D. H. and S. Ganguly, "An overview of fractal antenna engineering," *IEEE Antennas and Propagation Magazine*, Vol. 45, 38–57, 2003.
8. De Young, C. S. and S. A. Long, "Wideband cylindrical and rectangular dielectric resonator antennas," *IEEE Antennas and Propagation Letters*, Vol. 5, 426–429, 2006.
9. Long, S. A., M. W. Mcallister, and L. C. Shen, "The resonant cylindrical dielectric cavity antenna," *IEEE Trans. on Antennas and Propagation*, Vol. 31, No. 3, 406–412, 1983.
10. Petosa, A., *Dielectric Resonator Antenna Handbook*, Artech House Publishers, 2007.
11. De Young, C. S. and S. A. Long, "Investigation of dual mode wideband rectangular and cylindrical dielectric resonator antennas," *International Sym. on Antennas and Propagation Society*, Vol. 4B, 210–213, 2005.
12. Sebastian, M. T., *Dielectric Materials for Wireless Communication*, Elsevier, 2008.
13. Marneffe, T., http://users.swing.be/TGMSoft.
14. Tsachtsiris, G., C. Soras, M. Karaboikis, and V. Makios, "A reduced size fractal rectangular curve patch antenna," *IEEE Electromagnetic Compatibility International Symposium*, 912–915, Istanbul, May 2003.
15. CST GmbH 2006 CST Microwave Studio (r) User Mannual V.6.0, Darmstadt, Germany, (www.cst.de).